The GIVE ionospheric delay correction approach to improve positional accuracy of NavIC/IRNSS single-frequency receiver

Mehul V. Desai* and Shweta N. Shah

Department of Electronics Engineering, Sardar Vallabhbhai National Institute of Technology, Surat 395 007, India

The Navigation with Indian Constellation (NavIC)/ Indian Regional Navigation Satellite System (IRNSS) is an independent navigation system developed for the Indian subcontinent by the Indian Space Research Organisation (ISRO). The positional accuracy of this system is mainly affected by the ionosphere of the low-latitude equatorial Indian subcontinent, as large ionospheric gradients and intense irregularities are present in it. The objective of this study is to improve the positional accuracy of NavIC/IRNSS systems by applying ionospheric correction using the most suitable single-frequency model. The data to be analysed were collected from the NavIC/IRNSS receiver provided by the Space Applications Centre, ISRO. A comparative analysis between the dual-frequency model and single-frequency model (e.g. GIVE model, coefficient-based model) was performed on the data from the NavIC/ IRNSS receiver. Different ionospheric models were applied to compute ionospheric delay (ionodelay) on a quiet day ($3 < K_P < 5$). Our result shows that both the single-frequency Grid Ionosphere Vertical Error (GIVE) model and dual frequency model outperform remarkably compared to the traditional coefficient-based model. The GIVE model was also analysed on FAR categorized satellites for different stormy days of different months. It was observed that during stormy days also, the 3D position computed by applying the GIVE model was nearly the same as the dual-frequency model.

Keywords: Ionosphere, navigation systems tropospheric delay, positional accuracy.

THE Navigation with Indian Constellation (NavIC)/Indian Regional Navigation Satellite System (IRNSS) is an aboriginal navigation system developed by the Indian Space Research Organisation (ISRO). The NavIC/IRNSS system will provide positioning service with 10 m accuracy for civilian and the military users in India[1]. The NavIC/IRNSS consists of three Geostationary Earth Orbit (GEO) and four Geo Synchronous Orbit (GSO) satellites. The NavIC/IRNSS satellites broadcast the signal in L_5 band (1164.45–1188.45 MHz) and S band (2483.5–2500 MHz) with a carrier frequency of 1176.45 MHz (F1) and 2492.08 MHz (F2) respectively[2–4]. Currently, the NavIC/ IRNSS constellation is completed as all seven satellites, i.e. 1A, 1B, 1C, 1D, 1E, 1F and 1G are active in the orbit[5].

Internet of Things (IoT) will be a promising technology in the upcoming years, where the devices will be connected with each other through the internet. The future of Indian navigation will depend on NavIC/IRNSS, which can be coordinated with IoT for anytime, anywhere access, permit data back-up with NavIC/IRNSS support for mobile assistance. It will be useful to solve many navigation challenges such as traffic jam, road block, etc. The positional accuracy of such a system can be influenced by a number of factors, such as the geometry created between satellites, delay in the signal reception caused by the ionosphere and troposphere, multipath, the Doppler effect, clock drift and receiver noise. These effects may lead to position inaccuracy/miscalculation and may result in system failure. Hence, it is necessary to identify and mitigate it.

The effect of satellite geometry is measured by the factor of Dilution of Precision (DOP). The present authors have analysed various DOP parameters for NavIC/IRNSS and enhanced NavIC/IRNSS with GPS systems. It was observed that as the number of IRNSS satellites increased, the performance of DOP improved[3]. In this study, the delay parameters have been analysed because a small delay in the signal may significantly affect the user (receiver) location. The existence of large irregularities in the ionosphere causes an increase in delay of L_5 and S band signals received from NavIC/IRNSS satellites[6]. Hence, the results obtained after computing the received signals with higher ionospheric irregularities generate error in position measurements[7,8]. Here, the popular computational algorithms (like dual-frequency and single-frequency models) have been applied to mitigate the error due to ionospheric irregularities and improve the positioning accuracy. Table 1 provides a summary of such algorithms[9–18]. However, feasibility check of these algorithms for NavIC/ IRNSS has not been performed in real-time scenario.

A detailed survey was conducted on different ionodelay models described above for the NavIC/IRNSS system[6]. Here, different single-frequency algorithms were investigated, which eliminate the need for extra frequency used in the dual-frequency model. The NavIC/IRNSS

*For correspondence. (e-mail: mvd.svnit@gmail.com)

Table 1. Summary of ionospheric correction algorithms

Application	Algorithms	Reference
Global positioning system (GPS)	Dual frequency method, differential correction approach and single-frequency ionospheric delay	9, 10
GPS-aided GEO augmented navigation (GAGAN)	High accuracy and precision in civil aviation	11, 12
	Minimum mean square error	13
	Inverse distance weighted (IDW) with the Klobuchar model	14
	Planar fit model	14
	Kriging	15
	Spherical harmonic function	16
	Modified Klobuchar model for two-shell model	17
	Taylor series expansion	18
NavIC/IRNSS	Kalman filter	7, 8

broadcasts eight coefficients (four α and four β) based on the Klobuchar model[2]. It also provides 90 Ionospheric Grid Point (IGPs)-based on grid model correction parameters in the L_5 band[5]. Hence, ionospheric correction was applied using the dual-frequency model, grid-based Grid Ionosphere Vertical Error (GIVE) model and eight coefficients-based model on a quiet day ($3 < K_P < 5$) data, collected by the Accord NavIC/IRNSS receiver. It has been realized from the positional error comparison that the performance of the grid-based GIVE model is similar to the dual-frequency model, i.e. using the single-frequency model also we could achieve performance similar to the dual-frequency model.

The Fast Fourier Transform (FFT) Averaging Ratio (FAR) algorithm was applied by Kowsik *et al.*[19] to detect ionospheric anomalies. Here, the FAR algorithm is used to identify the NavIC/IRNSS satellites, which are affected more by the ionosphere. The algorithm calculates a decision variable for each satellite which is recognized on the basis of a threshold. The threshold is set using an inverse chi-squared distribution function[9]. Here, the performance of the GIVE model can only be checked for FAR-classified satellites because it is highly affected by the ionosphere and is used to estimate the position of the fixed location (21.16° lat, 72.78° long). The 3D position is computed in terms of Distance Root Means Square (DRMS), Circular Error Probable (CEP) and Spherical Error Probability (SEP) after correcting the ionospheric delay, tropospheric delay and clock drift for the IRNSS and IRNSS + GPS system. From the simulation results (ionodelay as well as 3D position of IRNSS), it can be inferred that GIVE and the dual-frequency models showed similar performance during stormy ($K_P > 5$) days. Therefore, applying the GIVE model for ionospheric correction will not only improve the positional accuracy, but also avoid an additional hardware cost of extra frequency. The positional accuracy can be improved by combining IRNSS with GPS system.

Isonospheric correction models

The ionospheric irregularities were more prominent in the latitude range ±15° to ±20° (ref. 20). A large gradient was observed in the ionosphere near the Indian subcontinent[6]. Hence, the NavIC/IRNSS system would perform better when the additional delay due to the ionosphere is calculated effectively using powerful models or methods in a real-time scenario. The amount of delay contributed by the ionosphere depends on the path-integrated density of free electrons present in it, called Total Electron Content (TEC). TEC changes throughout the day due to recombination and ionization processes. It also depends on the season, solar cycle and geographical location of the user[21]. The quiet and stormy days are identified by a variety of geomagnetic indices, such as K, K_P, A_P and D_{st}, and correlated with the variation of TEC in the ionosphere[22]. Since the ionosphere is a dispersive medium, the delay is different for different frequencies. The ionospheric delay for the NavIC/IRNSS system can be estimated proportional to TEC using the dual-frequency model given by eq. (1)[2,6]

$$\text{TEC (electrons/m}^2) = \frac{1}{40.3} \times \frac{F_1^2 * F_2^2}{(F_1^2 - F_2^2)} (P_1 - P_2), \qquad (1)$$

where P_1 and P_2 are pseudoranges measured in two frequencies $F_1(L_5)$ and $F_2(S)$ respectively. In the GPS system, normally coefficient-based Klobuchar model is applied for ionodelay computation. Here, coefficient-based correction is applied to NavIC/IRNSS, as described below.

Ionodelay computation using coefficient

The master frame of NavIC/IRNSS contains four sub-frames, where each sub-frame is 600 symbols long, contributing 2400 symbols per frames[2,6]. Sub-frames 1 and 2 transmit primary while sub-frames 3 and 4 transmit secondary navigation parameters respectively[1]. Secondary navigation parameters include ionospheric delay correction coefficient, ionospheric grid delays and confidence values. The ionodelay computation using coefficient is an empirical model which estimates the delay based on eight coefficients[8,13]. The coefficients are broadcast through

navigation data once a day. Depending on x parameter value mentioned in IRNSS Interface Control Document (ICD)[2], the ionospheric correction is applied at Ionospheric Pierce Point (IPP) as follows

If $x < 1.57$, then

$$T_{\text{iono}}(\text{m}) = F * \left[5.0 * 10^{-9} + A_I \left(1 - \frac{x^2}{2!} + \frac{x^2}{4!} \right) \right]. \quad (2)$$

Otherwise,

$$T_{\text{iono}}(\text{m}) = F * (5 * 10^{-9}), \quad (3)$$

where A_I is the amplitude computed based on four α correction coefficients received from the NavIC/IRNSS satellites. F is an obliquity factor (more details about this model are provided in ref. 2). The eight-coefficient model is simple, but because the correction factor is fixed on the day, it cannot work efficiently. When compared, the GIVE model is found to be more efficient.

Grid-based ionocorrection

The NavIC/IRNSS satellites broadcast grid correction information for 90 IGPs ($5° \times 5°$ grids over the Indian region) in the L_5 band[2]. The broadcast message includes a Grid Ionosphere Vertical Delay (GIVD), Grid Ionosphere Vertical Error Indicator (GIVEI), region ID (90 IGPs are divided into six regions), region masked and Issue of Data Ionosphere (IODI)[2,12]. The users receive 15 IGPs grid correction information depending on region ID, which is used to compute the ionospheric correction with the following.

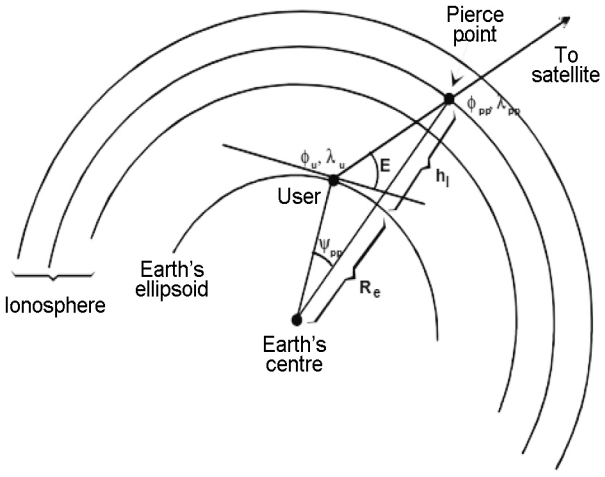

Figure 1. The user ionospheric pierce point location at 350 km above the earth's surface.

Step-1: Depending on A_z and E_l angles between NavIC/IRNSS satellite and user location (lat ϕ_u, long λ_u), IPP latitude and longitude ϕ_{pp} and λ_{pp} are calculated[2,9]. The IPP is at 350 km above the earth's surface and is in the line-of-sight (LOS) point between the satellite and the user[10,12] (Figure 1)

$$\psi_{\text{pp}}(\text{radian}) = \frac{\pi}{2} - E_l - \sin^{-1}\left[\left(\frac{R_{\text{e}}}{R_{\text{e}} + h} \right) * \cos(E_l) \right], \quad (4)$$

where R_{e} is the earth's radius, taken to be 6378.137 km and h is assumed to be 350 km.

$$\phi_{\text{pp}}(\text{radian}) = \sin^{-1}\left[\begin{matrix} \sin(\phi_u) * \cos(\psi_{\text{pp}}) + \\ \cos(\phi_u) * \sin(\psi_{\text{pp}}) * \cos(A_z) \end{matrix} \right], \quad (5)$$

and

$$\lambda_{\text{pp}}(\text{radian}) = \lambda_{\text{u}} + \sin^{-1}\left[\frac{\sin(\psi_{\text{pp}}) * \sin(A_Z)}{\cos(\phi_{\text{pp}})} \right]. \quad (6)$$

Step 2: IGPs are selected based on calculating the 3D position of users at IPP. Selection of IGPs has been done as follows[2,12].

- Check for four IGPs around IPP with GIVEI < 14.
- If one of the selected IGPs has GIVEI > 14, then discard the same and find the delay correction using three IGPs, but the location of IPP should be inside the triangle made by the three IGPs.
- If more than one of the selected IGPs have GIVEI > 14, then no ionospheric correction is required for the chosen IPP at the given time.

Step 3: Apply the interpolation on the GIVD value of the selected IGP (3 or 4) and calculate the User Ionospheric Vertical Error (UIVE) at the user IPP location[2,10,11]

$$\sigma_{\text{UIVE}}(\text{m}) = \sum_{n=1}^{4(\min 3)} W_n * X_{\text{pp}} * Y_{\text{pp}} * \sigma_{\text{GIVE}_n}.$$

Step 4: Ionospheric correction (IC) is applied at IPP as follows[2,16]

$$\text{IC}(\text{m}) = -\tau_{\text{spp}}(\phi_{\text{pp}}, \lambda_{\text{pp}}) = -F_{\text{pp}} * \tau_{\text{vpp}}(\phi_{\text{pp}}, \lambda_{\text{pp}}), \quad (8)$$

where τ_{spp} is the slant ionodelay and F_{pp} is the obliquity factor. In a grid-based model, corrections are updated every 288 s. Hence the GIVE model will be more efficient compared to the coefficient-based model. Due to the relative location of the IRNSS satellites, the signal from each satellite experiences a different amount of ionospheric delay. To classify the NavIC/IRNSS satellites

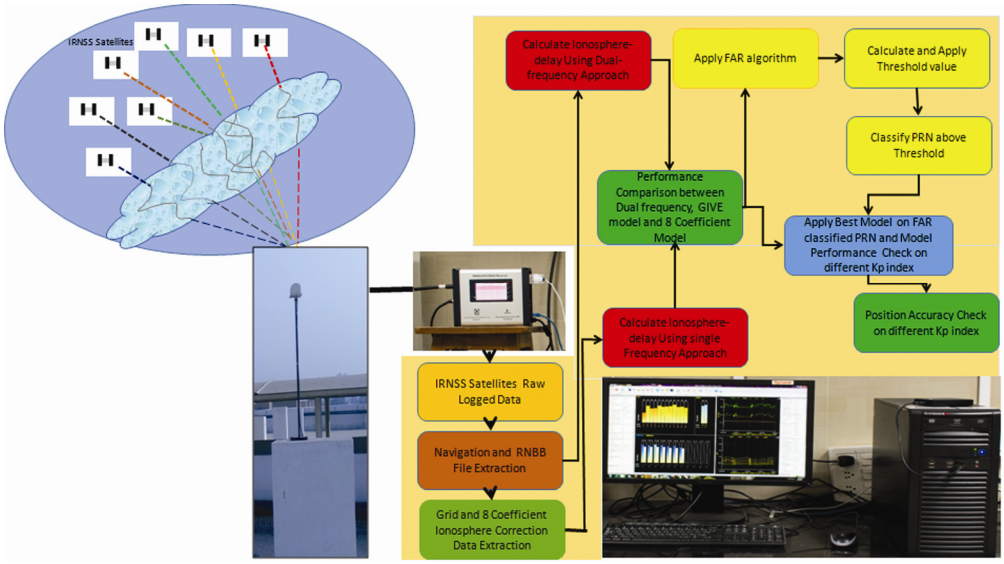

Figure 2. Experimental set-up of IRNSS/NavIC receiver and flow diagram of the methodology.

which are more affected by the ionospheric, the FAR algorithm is applied.

FAR algorithm

For analysis using the FAR algorithm, TEC data from each satellite were obtained from the ionospheric delay model and provided as an input to the algorithm. Let $a_n(t)$ be the variation in the TEC, where the data are taken at unit sample per second. Applying FFT to the input, we get[19]

$$A_n(s) = \sum_{l=0}^{L-1} a_k(l) * \exp(-j2\pi sl/L), \tag{9}$$

where l to $L-1$ denote the sample values and n to $N-1$, the number of satellites. Since the FFT output is symmetric, only the first half of the output $A_n(s)$ is considered ($s = 0$ to $L/2 + 1$ and $n = 0$ to N). The power spectral density (PSD) of $A_n(s)$ is found as follows

$$\text{PSD}_n\,(\text{s}) = |\, A_n(s)\,|^2 . \tag{10}$$

Now, for every segment, the average PSD (PSD_{avg}) and mean of PSD (PSD_{mean}) corresponding to each PRN are calculated. The decision criterion is defined by taking the ratio $\text{PSD}_{\text{avg}}/\text{PSG}_{\text{mean}}$.

$$D(n) = \frac{\text{PSD}_{\text{avg}}}{\text{PSD}_{\text{mean}}}. \tag{11}$$

In order to identify the satellite, the decision criterion is compared with the threshold. The classification is done by the following rule

$$D(n) > \gamma, \quad \text{disturbed}; \quad D(n) < \gamma, \quad \text{quiet}, \tag{12}$$

where γ is the threshold value.

Simulation and results

Let us now validate the theoretical analysis of all the models described above. The simulation tool MATLAB R.14 was used to estimate the ionospheric delay for the NavIC/IRNSS system. Data for various months were collected from the Accord NavIC/IRNSS receiver located at the Communication Research Laboratory, Electronics Engineering Department, Sardar Vallabhbhai National Institute of Technology (SVNIT), Surat (21.16° lat, 72.78° long), provided by the Space Applications Centre (SAC), ISRO, Ahmadebad. Figure 2 illustrates the experimental set-up of the NavIC/IRNSS system and the flow of implementation. The received data were sorted day-wise for each of the seven NavIC/IRNSS and other GPS satellites.

One week raw data of NavIC/IRNSS and GPS satellites starting from Time of Week Count (TOWC) 0 (starting on Sunday, 14 August 2016) to 648,000 (end of Saturday, 20 August 2016) were collected for analysis. We can choose, any range of dates. Here these dates were selected based on K_p index. The range between the NavIC/IRNSS satellites (1A–1G) and the user receiver was calculated by extracting primary information from the raw data. Initially, the range for L_5 and S bands was calculated followed by a dual frequency approach to measure the ionodelay for individual satellites. The results are discussed for a quiet day (14 August 2016) for ($3 < K_P < 5$). Figure 3 provides a comparison of ionodelay for six satellites (1B–1G). Data of satellite 1A were neglected as the receiver was unable to track the satellite.

At local noon, ionization maximizes; hence the recombination is slow and electron density maximizes soon after local noon (12.00–14.00 h). According to the literature, the dual-frequency approach always gave better performance, but at the cost of additional frequency. Here, the target was to reduce the cost of additional frequency and this was done by applying and comparing the performance of the various single-frequency models with the dual-frequency model.

The GIVE and coefficient models have been selected here. To apply the GIVE and coefficient-based models, we need 90 IGPs values and ionospheric correction coefficients, which were extracted from the raw navigation data. Figure 4 *a–f* shows the comparative performance estimation for NavIC/IRNSS 1B to 1G satellites of dual frequency, GIVE and coefficient-based models respectively. The GIVE and the dual-frequency models show similar performance; the former utilizes single frequency and the latter utilizes dual frequencies. The coefficient-based model gives the worst performance compared to the other two methods (Figure 4). Hence, dual frequency and GIVE models were considered for further analysis.

The FAR algorithm was applied to each satellite datum received on 14 August 2016 ($3 < K_P < 5$) to identify the effect of ionization. Figure 5 *a* and *b* shows the TEC data and FAR performance respectively. Figure 5 *a* is plotted for different TEC values for different NavIC/IRNSS satellites (1B–1G). It can be seen that on all days, the peak of the fourth (1D) and the seventh (1G) satellites is above a threshold value (decision variable). The lowest peak corresponds to the third satellite (1C) according to the decision variable. Hence, 1D and 1G are affected more due to the ionospheric variations throughout the analysed days (for the fixed location, 21.16° lat, 72.78° long) (Figure 5 *c*) and 1C is the least affected. This is due to the arrangement of the satellites shown as a skyplot (Figure 5 *d*). It describes the relative arrangement of the satellite constellation with respect to the receiver location. The signals from the fourth and seventh satellites have to traverse a longer distance through the ionosphere compared to the third satellite.

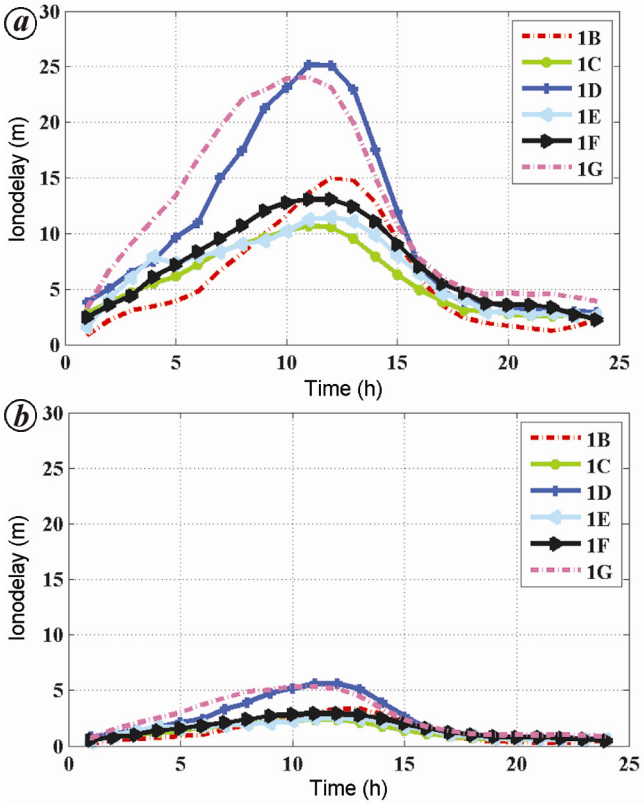

Figure 3. Dual frequency model analysis ((***a***) L_5 band ionodelay analysis and (***b***) *S*-band ionodelay analysis) on a quiet day, i.e. 14 August 2016 ($3 < K_P < 5$).

Figure 6 illustrates statistical analysis of ionospheric delay computed by different models on 14 August 2016 ($3 < K_P < 5$). The performance of the FAR (as shown in Figure 3) was verified by comparison with the statistical analysis of ionodelay (maximum, mean and standard deviation values) discussed in Figure 6. The calculated values of maximum ionodelay are 15, 11, 25, 11, 13 and 24 m for satellites 1B to 1G respectively. It can be observed that maximum ionospheric effect is experienced by satellites 1D and 1G. 1D provides higher delay among all the satellites with its value for L_5 and *S* bands being 25 and 6 m respectively. Considering the mean, 1G has a higher value (12 m for L_5 and 3 m for *S* band). Similarly, standard deviation for 1G in L_5 is 8 m and for 1D in *S* band is 2 m.

It can be observed from Figure 6 that the dual-frequency approach has a maximum delay for satellite 1D, which is around 25 m, whereas the GIVE and coefficient-based models provide maximum delay of 23 and 17 m respectively. Thus the performance of the GIVE and coefficient-based models is degraded by 2 and 8 m respectively, compared to the dual-frequency model. From these observations, we can conclude that the GIVE model may be used in place of the dual-frequency model, which provides similar performance. To verify the performance of GIVE, it is being tested for various other stormy days as well.

The GIVE performance was checked for various stormy days for only the FAR classified satellites, as it majorly affected by ionosphere due to its relative location with respect to the fixed receiver location (21.16° lat, 72.78° long). Figures 7–9 illustrate the ionodelay and statistical analysis of the dual-frequency and GIVE models for different stormy days (22 August 2016, 2 September 2016, 3 September 2016) with $K_P = 5$; 6; 6- and $A_P = 18$; 37; 36 respectively, where a large ingredient is present. The results show that the performance of the GIVE model is similar to that of the dual-frequency model in stormy day ($K_P > 5$) also.

The troposphere (60 km altitude) also adds additional delay to the IRNSS signal reception. The troposphere

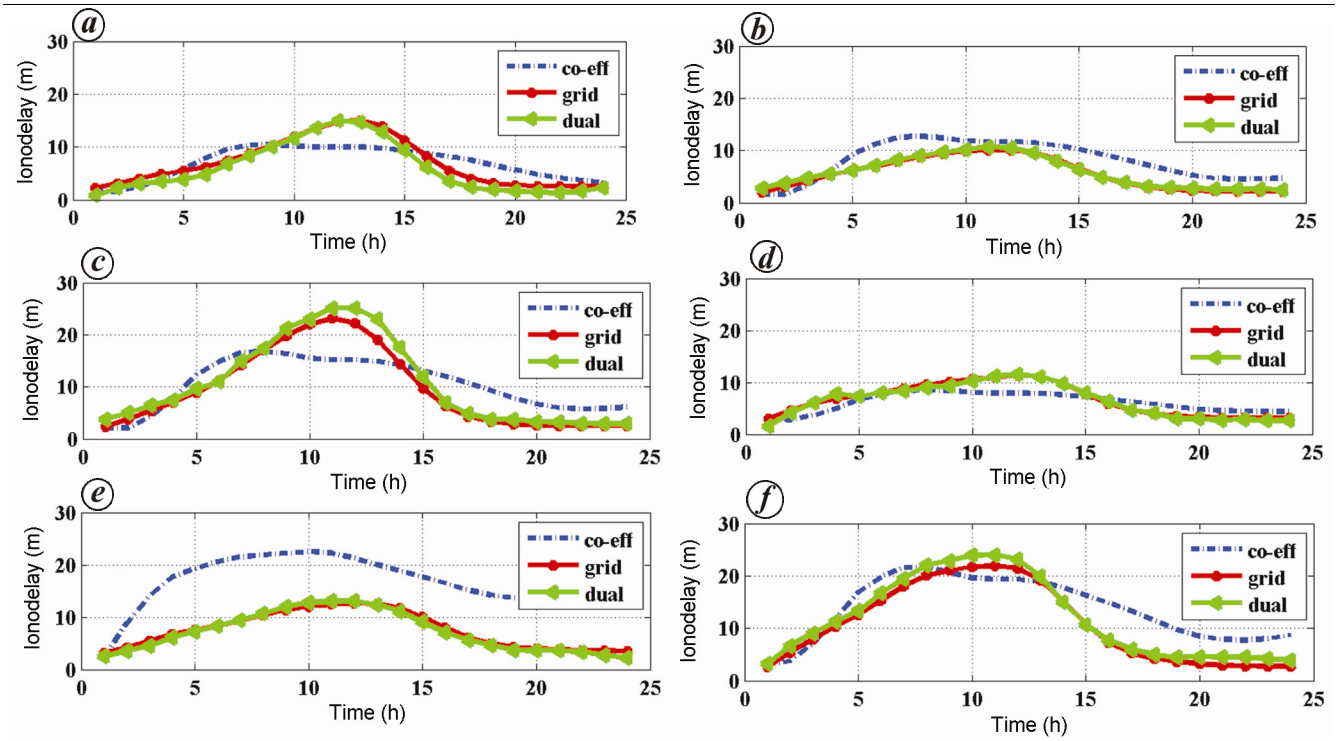

Figure 4. IRNSS/NavIC satellite (***a***, 1B; ***b***, 1C; ***c***, 1D; ***d***, 1E; ***e***, 1F; ***f***, 1G) ionospheric delay comparison (L_5 band) of different models on 14 August 2016 ($3 < K_P < 5$).

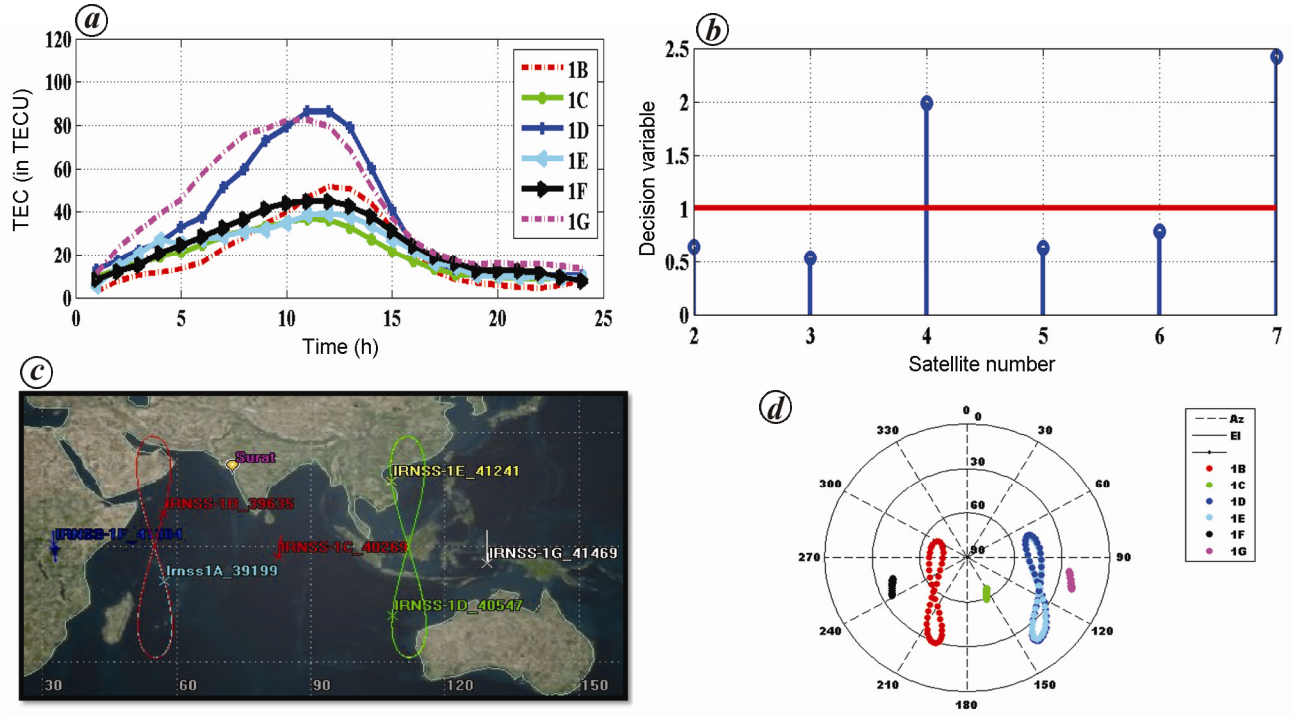

Figure. 5. IRNSS analysis on a quiet day, i.e. 14 August 2016: ***a***, TEC variation; ***b***, FAR algorithm analysis; ***c***, receiver location; ***d***, skyplot of IRNSS.

delay is mainly due to the presence of various drying gases, wet components in the form of water vapour and condensed water in the form of clouds. Various troposphere models are available which are navigation-oriented and more accurate[23,24]. Here, troposphere delay for the IRNSS L_5 band signal was estimated using the Hopfield model (Figure 10). Figure 11 provides the C/N_0 analysis of the IRNSS L_5 band signal. The 3D positional

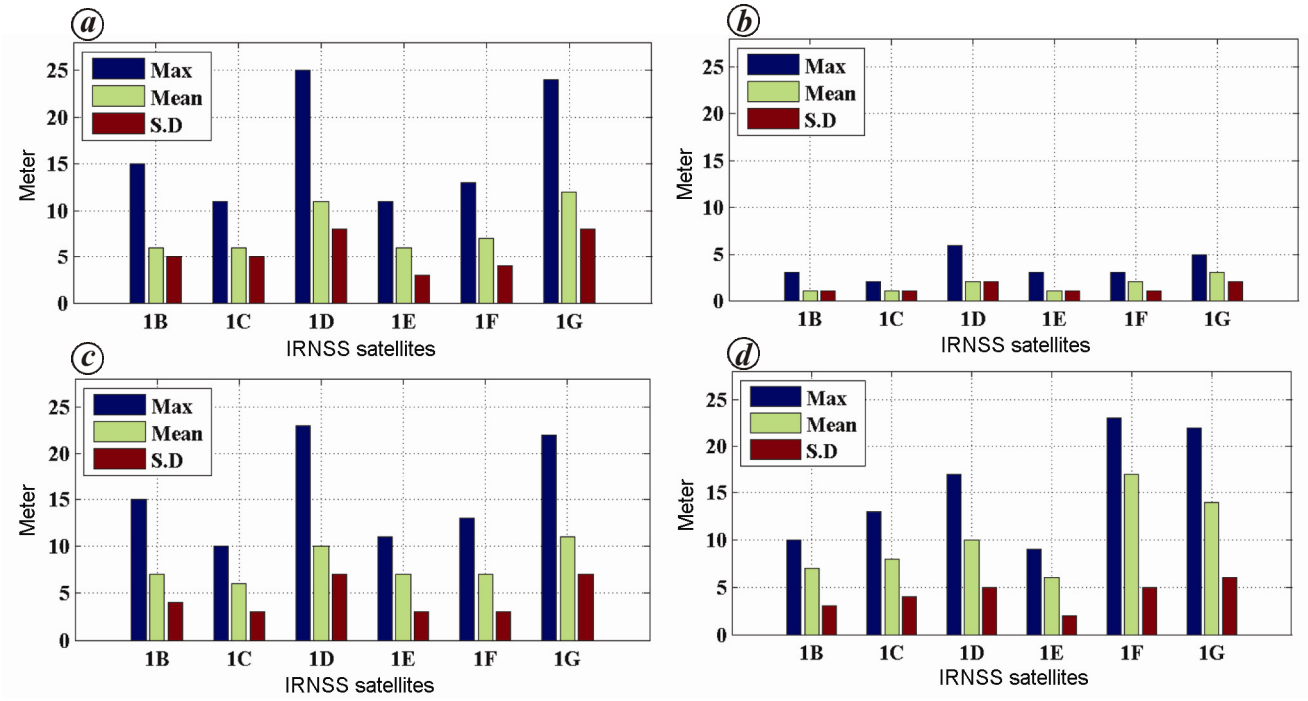

Figure 6. Statistical analysis of ionospheric delay computed by (***a***) dual L_5 band, (***b***) dual S band, (***c***) GIVE L_5 band and (***d***) Klobuchar L_5 band on 14 August 2016 ($3 < K_P < 5$).

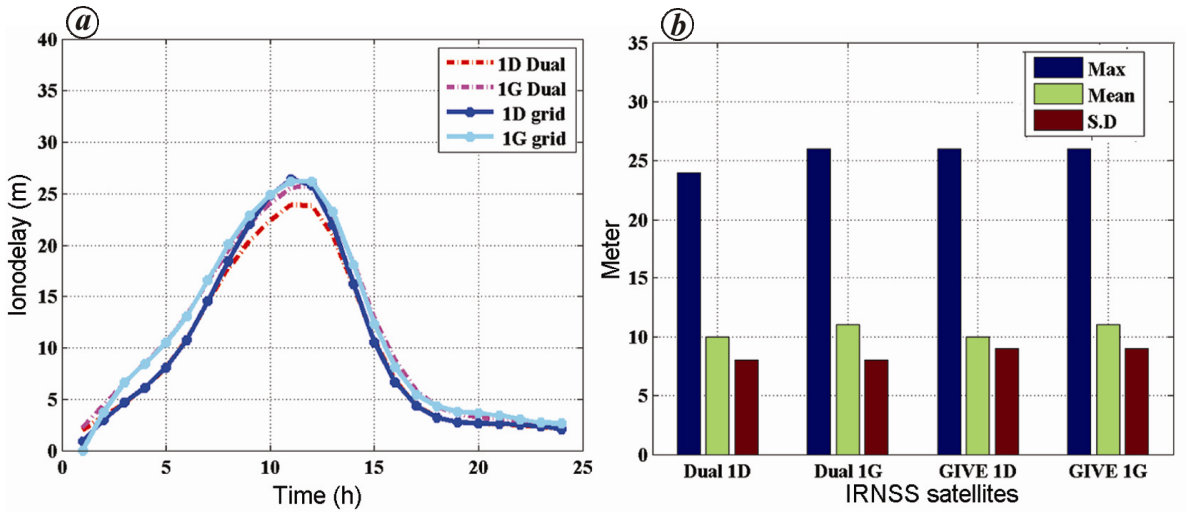

Figure 7. (***a***) Ionodelay and (***b***) statistical analysis comparison between dual frequency and GIVE models on 22 August 2016 ($K_P = 5$).

error in terms of Earth Centre Earth Fix (ECEF) coordinates was measured after correcting the ionospheric effect, tropospheric effect and satellite clock correction (Figure 12).

The 3D position was calculated by iterative least square (ILS) estimation algorithm[25]. Figure 12 *b* shows that when ionospheric correction is applied, the IRNSS position error is reduced compared to without correction (Figure 12 *a*). The IRNSS 3D positional error in terms of east, north and up coordinate system was computed on selected stormy days. The IRNSS 3D position was estimated for (i) without ionospheric correction, (ii) with dual-frequency correction and (iii) with GIVE correction (Figure 13) (22 August 2016, $K_P = 5$), Figure 14 (2 September 2016, $K_P = 6$) and Figure 15 (3 September 2016, $K_P = 6$) respectively). It has been observed that after the ionospheric correction, the positional accuracy of the IRNSS system is improved.

The behaviour of 3D position computed by applying GIVE correction was the same as that computed after dual-frequency correction. When the IRNSS system is combined with the GPS system, the positional accuracy can be improved further. The position accuracy was evaluated in terms of DRMS, CEP and SEP (Table 2). It has

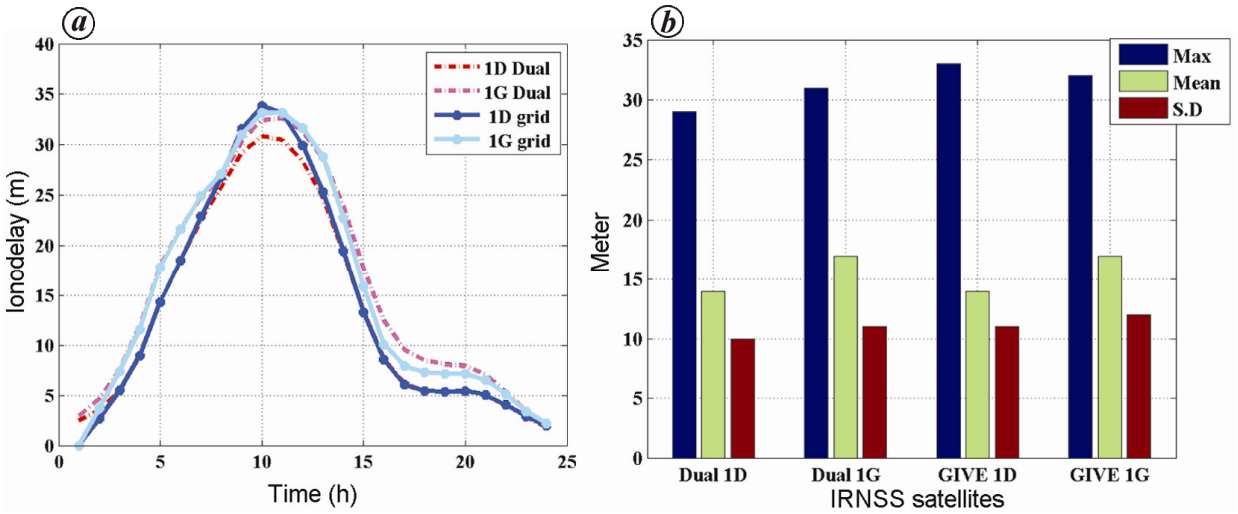

Figure 8. (*a*) Ionodelay and (*b*) statistical analysis comparison between dual frequency and GIVE model on 2 September 2016 (K_P = 6-).

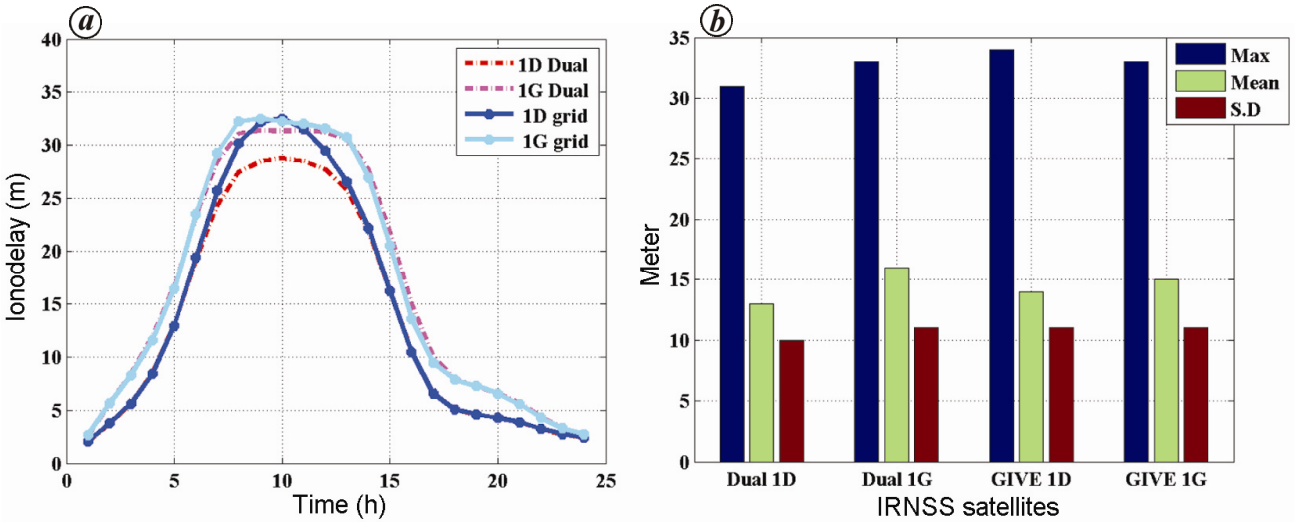

Figure 9. (*a*) Ionodelay and (*b*) statistical analysis comparison between dual frequency and GIVE model 3 September 2016 (K_P = 6-).

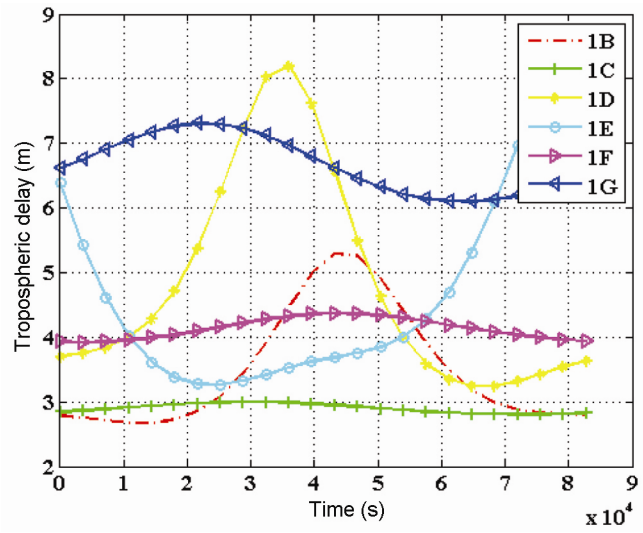

Figure 10. IRNSS L_5 band troposphere delay analysis.

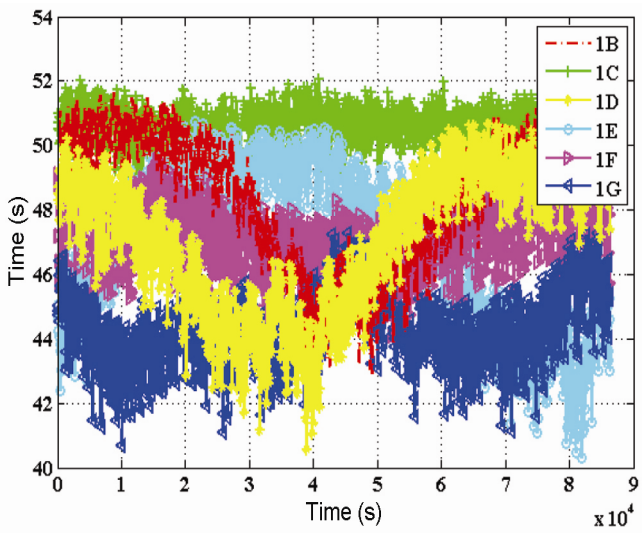

Figure 11. IRNSS L_5 band C/N_0 analysis.

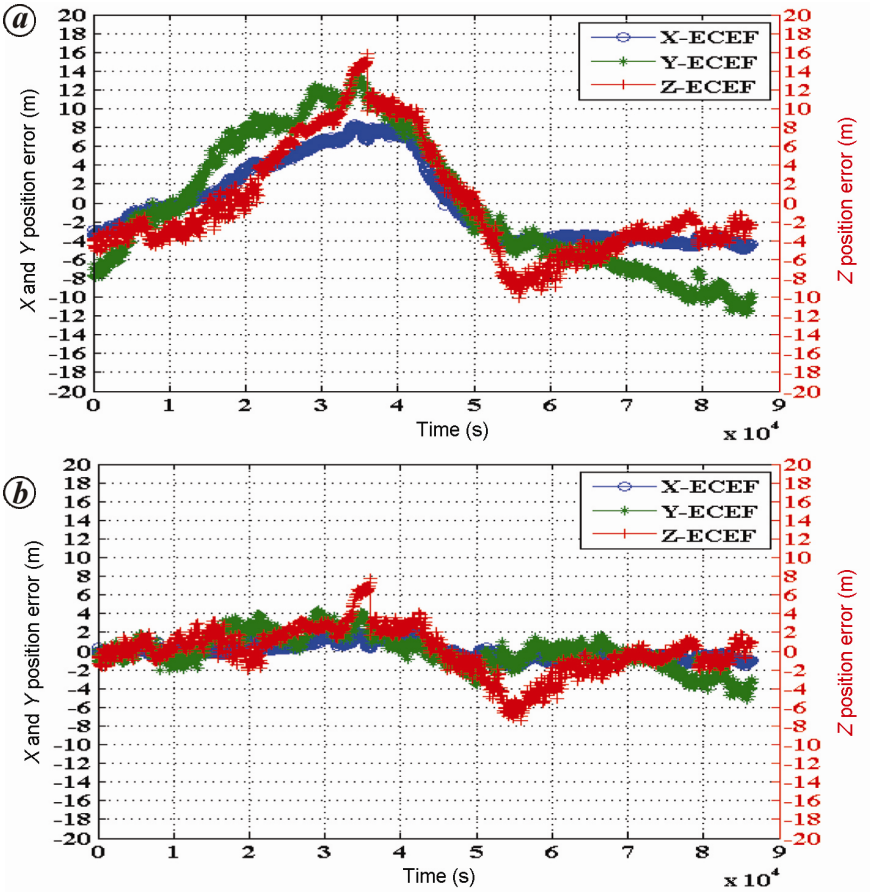

Figure 12. IRNSS position error (ECEF). (***a***) Without and (***b***) with ionospheric correction.

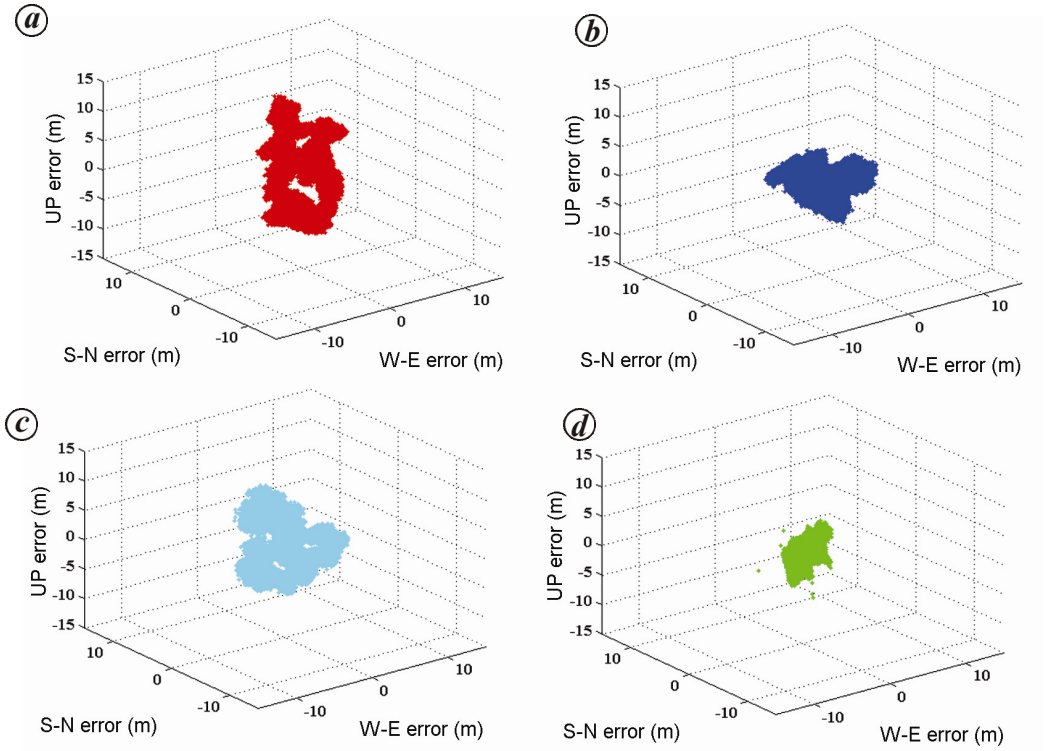

Figure 13. Position error: ***a***, IRNSS without ionospheric correction; ***b***, IRNSS with dual-frequency correction; ***c***, IRNSS with GIVE correction; ***d***, IRNSS + GPS with correction on 22 August 2016 (K_P = 5, A_P = 18).

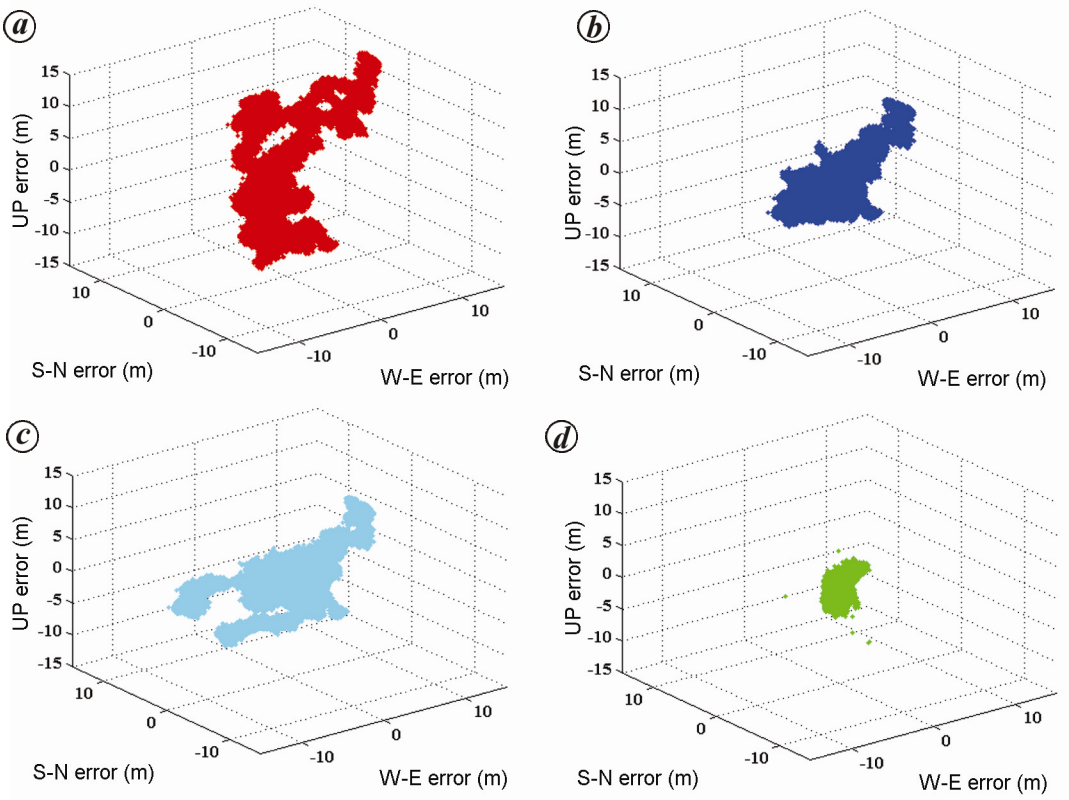

Figure 14. Position error. ***a***, IRNSS without ionospheric correction. ***b***, IRNSS with dual frequency correction. ***c***, IRNSS with GIVE correction. ***d***, IRNSS + GPS with correction on 2 September 16 (K_P = 6-, A_P = 37).

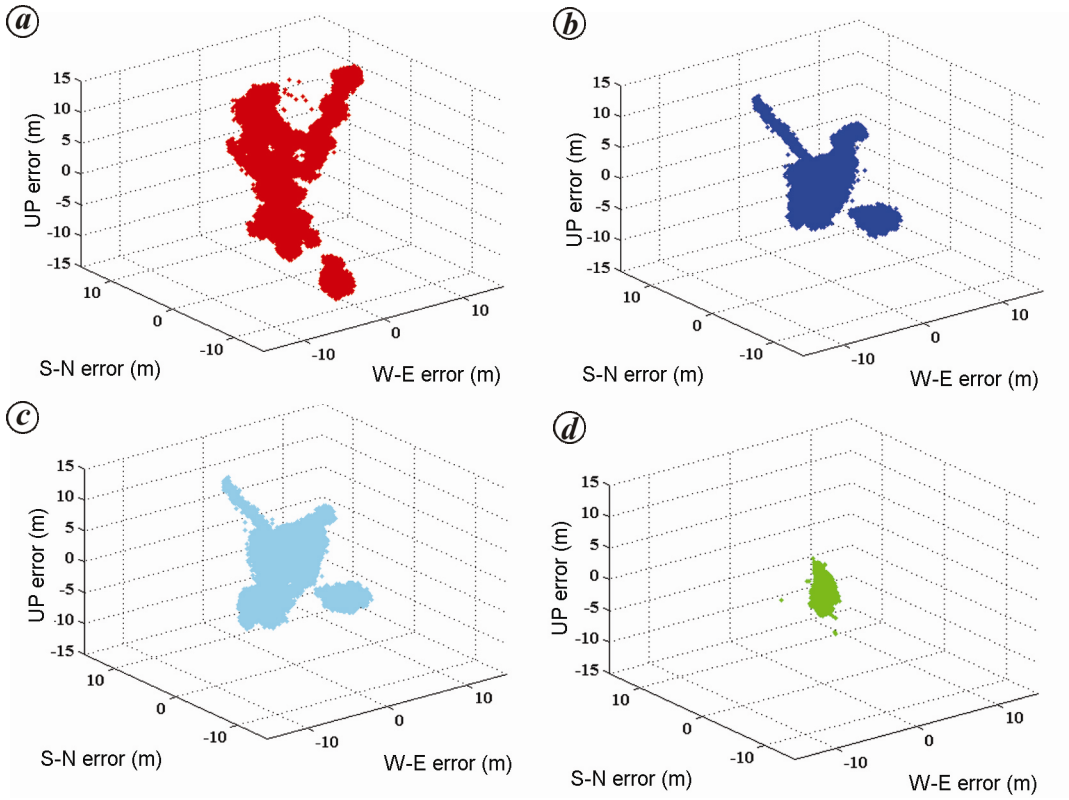

Figure 15. Position error. ***a***, IRNSS without ionospheric correction. ***b***, IRNSS with dual-frequency correction. ***c***, IRNSS with GIVE correction. ***d***, IRNSS + GPS with correction on 3 September 2016 (K_P = 6, A_P = 36).

Table 2. The statistical positional error analysis

Date	Parameters (m)	IRNSS	IRNSS dual frequency	IRNSS-GIVE	IRNSS + GPS
22 August 2016, $K_P = 5$, $A_P = 18$	3DRMS (mean)	16.0644	8.871	11.570	2.318
	CEP (mean)	4.1411	1.643	2.939	0.578
	SEP (mean)	4.7619	2.022	3.383	0.708
2 September 2016, $K_P = 6$, $A_P = 37$	3DRMS (mean)	25.187	7.501	8.969	3.676
	CEP (mean)	6.508	1.932	2.3246	0.959
	SEP (mean)	7.295	2.794	3.514	1.198
3 September 2016, $K_P = 6$-, $A_P = 36$	3DRMS (mean)	29.673	9.569	11.187	2.613
	CEP (mean)	7.560	2.353	2.785	0.662
	SEP (mean)	7.564	2.818	3.516	0.830

been observed that in terms of 3DRMS, CEP and SEP, the performance of IRNSS with ionospheric correction was found to be better. The performance of IRNSS with GIVE correction was nearly the same as the dual correction, with a cost of approximately 2–3 m for 3DRMS, 0.5–1.3 m for CEP and 0.8–1.4 m for SEP. The performance of IRNSS + GPS was best among all the combinations.

Conclusion

This study provides a comparative analysis of different ionospheric models to improve the positional accuracy of future NavIC/IRNSS systems. Initially, the ionospheric delay was calculated using the dual-frequency method, and then the optimal single-frequency model was found for the ionospheric correction. Performance comparison between the dual-frequency model, the single-frequency GIVE model and eight-coefficient model was made for a quiet day, i.e. 14 August 2016 ($3 < K_P < 5$). It has been observed that the GIVE model provides better performance compared to the coefficient-based model for all satellites. The FAR algorithm is able to distinguish the satellites that are affected by large variations due to the ionosphere. The results obtained are in agreement with those of the TEC data associated with each satellite. The GIVE model performance was also verified on different stormy days ($K_P > 5$). It has been observed that the position computed (3DRMS, CEP and SEP) after the GIVE correction and dual-frequency correction was approximately the same, based on single-frequency and dual-frequency approach respectively. Use of the GIVE model for ionospheric correction has not only improved the performance of the NavIC/IRNSS receiver, but has also reduced the cost of extra frequency with 1 m of error tolerance.

1. Thoelert, S., Montenbruck, O. and Meurer, M., IRNSS-1A: signal and clock characterization of the Indian regional navigation system. *GPS Sol.*, 2014, **18**(1), 147–152.
2. IRNSS signal in space ICD 2011, ISRO-ISAC V 1.1; http://www.isro.gov.in/irnss-programme/ (accessed on 7 March 2017).
3. Desai, M. V., Jagiwala, D. and Shah, S. N., Impact of dilution of precision for position computation in Indian Regional Navigation Satellite System. In Proceedings of the IEEE International Conference on Advances in Computing, Communications and Informatics, Jaipur, 2016, pp. 980–986.
4. Ruparelia, S., Lineswala, P., Jagiwala, D., Desai, M. V., Shah, S. N. and Dalal, U. D., Study of L5 band interferences on IRNSS. In Proceedings of the International Conference on Global Navigation Satellite System (GPS-aided GEO augmented navigation-IRNSS), User Meet, Bengaluru, 2015.
5. http://www.isro.gov.in/Applications/Satellite Navigation Program/ (accessed on 7 September 2017).
6. Desai, M. V. and Shah, S. N., Ionodelay models for satellite based navigation system. *Afr. J. Comput. ICT*, 2015, **8**(2), 1–6.
7. Rethika, T., Nirmala, S., Rathnakara, S. C. and Ganeshan, A. S., Ionospheric delay estimation during ionospheric depletion events for single frequency users of IRNSS. *Innov. Syst. Design Eng.*, 2015, **6**(2), 98–107.
8. Rethika, T., Mishra, S., Nirmala, S., Rathnakara, S. C. and Ganeshan, A. S., Single frequency ionospheric error correction using coefficients generated from regional ionospheric data for IRNSS. *Indian J. Radio Space Phys.*, 2013, **42**, 125–130.
9. Klobuchar, J. A., Ionospheric time-delay algorithm for single-frequency GPS users. *IEEE Trans. Aerospace Electron. Syst.*, 1987, **3**, 325–331.
10. Andrei, C. O., Chen, R., Kuusniemi, H., Hernandez-Pajares, M., Juan, J. M. and Salazar, D., Ionosphere effect mitigation for single frequency precise point positioning. In Institute of Navigation, Global Navigation Satellite System, 2009, pp. 2508–2517.
11. Prasad, N. and Sarma, A. D., Preliminary analysis of grid ionospheric vertical error for GAGAN. *GPS Sol.*, 2007, **11**(4), 281–288.
12. Acharya, R., Nagori, N., Jain, N., Sunda, S., Regar, S., Sivaraman, M. R. and Bandopadhyay, Ionospheric studies for the implementation of GAGAN. *Indian J. Radio Space Phys.*, 2007, **36**, 394–404.
13. Ratnam, D. V. and Sarma, A. D., Modeling of Indian ionosphere using MMSE estimator for GAGAN applications. *J. Indian Geophys. Union*, 2006, **10**(4), 303–312.
14. Sarma, A. D., Venkata Ratnam, D. and Krishna Reddy, D., Modelling of low-latitude ionosphere using modified planar fit method for GAGAN. *IET J. Radar, Sonar Navigat.*, 2009, **3**(6), 609–619.
15. Venkata Ratnam, D., Sarma, A. D., Satya Srinivas, V. and Sreelatha, P., Performance evaluation of selected ionospheric delay models during geomagnetic storm conditions in low latitude region. *Radio Sci.*, 2011, **46**(3), 1–7.

16. Venkata Ratnam, D. and Sarma, A. D., Modeling of low-latitude ionosphere using GPS data with SHF model. *IEEE Trans. Geosci. Remote Sensing*, 2012, **50**(3), 972–980.
17. Shukla, A. K., Das, S., Shukla, A. P. and Palsule, V. S., Approach for near-real-time prediction of ionospheric delay using Klobuchar-like coefficients for Indian region. *IET J. Radar, Sonar Navigat*., 2013, **7**(1), 67–74.
18. Kumar, P. N., Sarma, A. D. and Reddy, A. S., Modelling of ionospheric time delay of global positioning system (GPS) signals using Taylor series expansion for GPS-aided geo augmented navigation applications. *IET J. Radar, Sonar Navigat*., 2014, **8**(9), 1081–1090.
19. Kowsik, J., Bhanu Kumar, T., Mounika, G., Venkata Ratnam, D. and Raghunath, S., Detection of ionospheric anomalies based on FFT averaging ratio (FAR) algorithm. In Proceedings of the International Conference in Innovations in Information, Embedded and Communication Systems, 2015, pp. 1–3.
20. Raghunath, S. and Venkata Ratnam, D., Detection of low-latitude ionospheric irregularities from GNSS observations. *IEEE J. Appl. Earth Obser. Remote Sensing*, 2015, **8**(11), 5171–5176.
21. Panda, S. K., Gedam, S. S. and Jin, S., Ionospheric TEC Variations at low latitude Indian region. INTECH Open science, 2015, pp. 149–174.
22. http://www.swpc.noaa.gov/phenomena/coronal-mass-ejections// (accessed on 7 March 2017).
23. Saastamoinen, J. J., Simplified model for calculation of devolatilization in fluidized beds. *Fuel*, 2006, **85**(17), 2388–2395.
24. Hopfield, H. S., Tropospheric effect on electromagnetically measured range. Prediction from surface weather data. *Radio Sci.*, 1971, **6**(3), 357–367.
25. He, Y. and Bilgic, A., Iterative least squares method for global positioning system. *Adv. Radio Sci*., 2011, **9**, 203–208.

ACKNOWLEDGEMENT. We thank the Director, Group Head DCTG SNAA and scientists of the Space Applications Centre, ISRO, Ahmedabad for guidance.

Received 16 September 2017; accepted 9 November 2017

doi: 10.18520/cs/v114/i08/1665-1676